High-precision measurements of the diamond Hugoniot in and above the melt region

D. G. Hicks,[1,*] T. R. Boehly,[2] P. M. Celliers,[1] D. K. Bradley,[1] J. H. Eggert,[1] R. S. McWilliams,[1,3] R. Jeanloz,[3] and G. W. Collins[1]

[1]*Lawrence Livermore National Laboratory, Livermore, California 94550, USA*

[2]*Laboratory for Laser Energetics, University of Rochester, New York 14623, USA*

[3]*University of California, Berkeley, California 94720, USA*

(Received 15 August 2008; published 4 November 2008)

High-precision measurements of the diamond principal Hugoniot have been made at pressures between 6 and 19 Mbar. Shock velocities were determined with 0.3%–1.1% precision using a velocity interferometer. Impedance-matching analysis, incorporating systematic uncertainties in the equation of state of the quartz standard, was used to determine the Hugoniot with 1.2%–2.7% precision in density. The results are in good agreement with published *ab initio* calculations, which predict a small negative melt slope along the Hugoniot, but disagree with previous laser-driven shock wave experiments, which had observed a large density increase in the melt region. In the extensive solid-liquid coexistence regime between 6 and 10 Mbar, the present measurements indicate that the mixed phase is a few percent more dense than what would be expected from a simple interpolation between liquid and solid Hugoniots.

DOI: 10.1103/PhysRevB.78.174102 PACS number(s): 52.50.Lp

I. INTRODUCTION

Carbon has the highest melting or sublimation temperature (~4000 K) of any element at low pressures, a manifestation of its unusually large cohesive energy.[1,2] The diamond phase, with its apparently open yet compact structure, is stable up to extremely high pressures and remains the only observed high-pressure phase of carbon. Such compactness and stability is attributable to carbon's lack of core *p* electrons, which allows valence *p* electrons closer to the nucleus and creates particularly strong sp^3 bonds.[3] The study of diamond melting at high pressures, therefore, provides a valuable window into the limiting behavior of strongly bonded materials.

After early predictions by Bundy[4]—who suggested that the melt line of diamond, in analogy with that of Si and Ge, has a negative slope—shock experiments by Shaner *et al.*,[5] along with numerous models,[6–8] indicated instead that the melt line is positive. With an improved understanding of the structure of liquid carbon, predictions showed that diamond, like graphite, has a maximum in the melt line near 5 Mbar.[9–12] The diamond phase is calculated to be stable up to around 11 Mbar, above which the BC8 phase is favored,[9,12,13] although this new phase has yet to be observed.

The high-pressure melt line of diamond can be accessed experimentally using strong shock waves. The graphite Hugoniot crosses the positive slope region of the diamond melt line,[5,14] while the diamond Hugoniot, starting at a higher density, has been predicted by recent studies to cross the negative slope region. Calculations of the diamond Hugoniot by Correa *et al.*[9,15] using density-functional-based molecular-dynamics calculations indicate that melting along the diamond Hugoniot extends over an unusually large solid-liquid coexistence regime between 6 and 10 Mbar, crossing the diamond-BC8-liquid triple point at 9 Mbar (see for example Fig. 14 in Ref. 15 for a pressure versus temperature plot of the Hugoniot and its relation to the diamond and BC8 melt lines). Romero and Mattson[16] predicted a similar Hugoniot using the phase boundaries given by Wang *et al.*[10] and Correa *et al.*[9] to determine the melt region. Optical reflectivity measurements by Bradley *et al.*[17] showed that shocked diamond increases in conductivity between 6 and 10 Mbar, consistent with the continuous transition into a liquid metal.

Measurements of the diamond Hugoniot in its solid phase were performed by Pavlovskii[18] and Kondo and Ahrens.[19] Much higher pressures were studied by Nagao *et al.*[20] and Brygoo *et al.*[21] using laser-driven shocks. Brygoo *et al.*[21] observed a dramatic increase in density at around 7.5 Mbar, suggesting a large negative melt slope. This distinct feature was not found in *ab initio* calculations,[15,16] raising the interesting possibility that the slope of the diamond melt line is significantly more negative than predicted. Ultimately, however, most of the laser-driven shock wave measurements of Nagao *et al.*[20] and Brygoo *et al.*[21] have significant error bars and do not tightly constrain the equation of state (EOS) of carbon near the diamond melt line.

In this paper, significantly higher precision measurements of the diamond Hugoniot in and above the melt region are described. The results are generally in agreement with *ab initio* predictions and suggest a small density increase at melting. In Sec. II details of the experimental apparatus are described. Section III describes the improvements that allowed particularly high-precision velocity measurements to be made. Section IV outlines the impedance-matching (IM) calculations. Section V shows the results. Section VI compares these results with previous measurements and theories.

II. EXPERIMENT

The experiment was performed on the OMEGA laser facility at the University of Rochester, a neodymium-doped phosphate glass system operating with frequency-tripled, 0.35-μm light.[22] To generate the shock pressures explored in these experiments, laser energies between 300 and 1000 J were delivered using a nominally square pulse of either 2 or 3 ns in duration. The laser focal spot was smoothed using

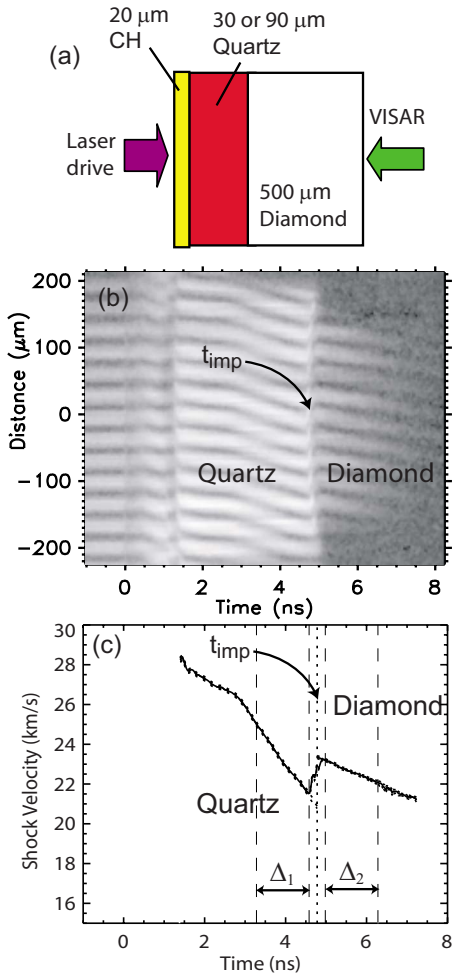

FIG. 1. (Color online) (a) Schematic of the quartz-diamond impedance-matching targets. (b) Line VISAR trace showing reflecting shock fringes in quartz and diamond. The time that the shock crosses the interface between the two materials is labeled as t_{imp}. The shock crosses the CH ablator between 0 and 1.25 ns. (c) Velocity history extracted from the VISAR trace in (b); dotted lines above and below the lineout indicate measurement errors; t_{imp} is the instant at which the impedance-matching velocities are taken. To precisely determine the velocity at t_{imp}, a linear fit is taken of the velocities over a neighboring time interval Δ_1 (or Δ_2) and extrapolated forward (or backward) to t_{imp}.

distributed phase plates, producing near uniformly irradiated spots of either 600 or 800 μm in diameter, depending on the experiment. This resulted in average laser intensities between 3 and 9×10^{13} W/cm^2.

Targets consisted of $>$150-μm-thick type Ia or IIa diamond oriented along the (110) axis and glued onto either a 20–30-μm- or 80–90-μm-thick z-cut α-quartz sample [see Fig. 1(a)]. The quartz was used as the reference standard for the impedance-matching measurement. The glue layer was kept below 2-μm thick. The other side of the quartz, illuminated by the laser drive, had a 20-μm CH ablator to reduce hard x-ray generation. The free surface of the diamond had an antireflective coating to minimize back reflections. The diamond and quartz densities were 3.51 g/cm^3 and 2.65 g/cm^3, respectively. At the probe laser wavelength of 532 nm, the index of refraction of the diamond and quartz samples were 2.42 and 1.55, respectively.

Shock velocities in the quartz and diamond samples were measured using a line-imaging velocity interferometer system for any reflector (VISAR) (Refs. 23–26), which measures the Doppler shift of a moving reflector. By design, drive pressures were kept sufficiently high in these experiments that the shock front was optically reflecting in quartz[27] and diamond,[17] allowing the VISAR to provide a direct, time-resolved measurement of the shock velocity in both materials. Two VISARs were run concurrently on each shot, the first using an 18-mm etalon and the second using a 7-mm etalon.[28] This corresponds, respectively, to velocity sensitivities of 1.766 and 4.465 μm/ns/fringe for quartz and 1.129 and 2.854 μm/ns/fringe for diamond. Only measurements from the high-sensitivity VISAR were used in the analysis; the less sensitive VISAR was used to resolve the 2π phase-shift ambiguities, which occur at shock breakout. Post processing of the VISAR images using Fourier transform methods determines the fringe position to $\sim$5% of a fringe, with larger errors being incurred on shots with particularly low shock reflectivities; the resulting velocities were measured to 0.3%–1.1% precision since shock speeds were high enough to cause multiple fringe shifts. The probe source for the VISAR was an injection-seeded, Q-switched, yttrium-aluminum garnet laser, operating at a wavelength of 532 nm. Streak cameras with temporal windows of 9 and 15 ns were used to detect the reflected probe signal. The time resolution of the diagnostic was dominated by the 90 or 40 ps delay time in each interferometer.

Twelve shots were taken at diamond pressures between 6 and 19 Mbar. Below 6 Mbar the shock front in diamond is no longer optically reflecting,[17] making it impossible to perform the highly precise VISAR measurements of the shock velocity. As will be shown, at pressures much above 19 Mbar in diamond (corresponding to $\sim$15 Mbar in quartz), systematic uncertainties in the quartz reference standard make it difficult to perform highly accurate measurements.

III. HIGH-PRECISION VELOCITY MEASUREMENTS

A significant improvement in the precision of velocity measurements was achieved in this experiment compared to that in most of the previous laser-driven shock wave experiments on diamond.[20,21] This improvement was accomplished in part by using quartz as an impedance-matching standard, thus, allowing a completely VISAR-based measurement of shock velocities and eliminating the need for the less precise transit-time measurements. A similar scheme has been implemented on several recent experiments.[29–31] A subset of the diamond Hugoniot measurements by Brygoo *et al.*[21] also used this same technique, although the present measurements were performed with a more sensitive interferometer.

Use of the VISAR to measure shock velocities in a quartz standard also solved the problem posed by unsteady laser-driven shock waves. Since unsteady shocks can vary in velocity by several percent over typical transit-time intervals of 1–2 ns, this is a large, and potentially difficult to quantify, source of error. Using the time-resolved VISAR measure-

ment allowed velocities to be tracked continuously during transit through the samples; values immediately before and after the shock crossed the quartz-diamond interface were then used in the impedance-matching analysis (see below).

It is important to recognize that while the presence of a nonsteady wave can severely compromise a transit-time measurement, it does not compromise the validity of the impedance-matching method itself. The impedance-matching construct relies on the condition that the pressure and particle velocities are continuous across the common interface between two materials. These materials undergo shock, reshock, or release at the instant the shock crosses the interface in order to maintain this condition. Such behavior follows immediately from mass and momentum continuities across an interface and is true whether or not the shock is steady. The complication for unsteady waves is one of measurement accuracy: measured shock velocities must be determined immediately before and after the shock transits the interface if they are to be associated with the impedance-matched states.

The sample VISAR trace shown in Fig. 1(b) and the accompanying velocity lineout in Fig. 1(c) illustrate how the shock velocity is tracked continuously through the quartz and diamond samples. Even with this highly time-resolved velocity measurement however, small corrections are still required to accurately determine the shock velocity at the instant the shock wave crosses the interface. This is because, as seen in Fig. 1(c), when the shock transits the quartz-diamond interface the velocity change is not instantaneous. A short transition interval of ~300 ps is caused by (i) the finite time resolution of the VISAR and (ii) the presence of a ~1–2-μm glue layer at the interface. To account for this, velocities at the "instant" (t_{imp}) the shock crosses the interface are determined by linearly fitting velocities in a brief interval just before and after this blurred transition period [shown as Δ_1 and Δ_2 in Fig. 1(c)] and by extrapolating the fits to t_{imp} positioned at the center of the transition [given by the dotted line in Fig. 1(c)]. Errors in these extrapolations are included in the uncertainty analysis. This type of analysis can be compromised if there is a sudden increase in the drive pressure that causes a change in the shock velocity around the time when the wave crosses the interface. To avoid this problem these experiments often employed a gently decaying shock wave that attenuates smoothly in time.

IV. IMPEDANCE-MATCHING ANALYSIS

Impedance matching[32,33] is used to determine the diamond particle velocity (U_{pC}), pressure (P_C), and density (ρ_C) from the measured shock velocities in quartz, U_{sQ}, and diamond, U_{sC}. An IM method using the experimentally derived principal Hugoniot and a constant Gruneisen parameter has been developed for quartz and is described elsewhere.[34] For completeness, several of the salient details are described in this section. This analysis was used in the diamond Hugoniot measurements by Brygoo *et al.*[21] Systematic errors based on uncertainties in the quartz Hugoniot and the Gruneisen parameter are propagated throughout.

The quartz principal Hugoniot was measured previously[35] and found to have linear U_s-U_p behavior given by $U_s = a_0 + a_1(U_p - \beta)$, where $a_0 = 20.57 \pm 0.15$, $a_1 = 1.291 \pm 0.036$, and $\beta = 12.74$. Errors include measurement uncertainties as well as systematic uncertainties in the aluminum EOS used in the analysis of the quartz data.[36]

The quartz reshock Hugoniot is quite well approximated by a reflection of the principal Hugoniot in the P-U_p plane since the increase in shock pressure upon transit from the quartz into the diamond is only 20%–30%. Small deviations from this reflected Hugoniot behavior are estimated using the Gruneisen parameter, Γ, which determines the pressure difference between equal-volume states on the double- and single-shock Hugoniots. Using the shock Hugoniot relations and the thermodynamic definition of the Gruneisen parameter, the pressure on the quartz second shock Hugoniot, $P_{\mathrm{H2}}(v)$, at a given volume, v, is given by

$$P_{\mathrm{H2}}(v) = P_{\mathrm{H1}}(v) + (2v/\Gamma + v - v_1)^{-1} \times \{[P_{\mathrm{H1}}(v_1) - P_0](v_0 - v) + [P_{\mathrm{H1}}(v) - P_0](v_1 - v_0)\}, \quad (1)$$

where $P_{\mathrm{H1}}(v)$ is the corresponding pressure on the single-shock Hugoniot at volume v. The second shock originates from a first shock state of volume v_1 and pressure $P_{\mathrm{H1}}(v_1)$, with P_0 and v_0 being the unshocked pressure and volume, respectively. Further use of the Hugoniot relations shows that the particle velocity on the second shock Hugoniot, $U_{p\mathrm{H2}}(v)$, is given by

$$U_{p\mathrm{H2}}(v) = U_{p\mathrm{H1}}(v_1) \pm \sqrt{[P_{\mathrm{H2}}(v) - P_{\mathrm{H1}}(v_1)](v_1 - v)}, \quad (2)$$

where $U_{p\mathrm{H1}}(v_1)$ is the particle velocity of the single-shock state from which the second shock originates. In this experiment, the sign of the square root is always negative since the reshock is backward propagating.

Impedance matching requires that the quartz reshock pressure and velocity given by Eqs. (1) and (2) are related directly to the measured diamond shock velocity, U_{sC}, via the Hugoniot expression

$$P_{\mathrm{H2}}(v) = P_0 + \rho_{0C} U_{sC} U_{p\mathrm{H2}}(v), \quad (3)$$

where ρ_{0C} is the initial density of diamond. Since the quartz shock speed is measured, and, thus, $P_{\mathrm{H1}}(v_1)$ and v_1 are known, these equations can be solved for the single unknown v and then used to determine the pressure, particle velocity, and density of diamond.

The value of the Gruneisen parameter in strongly shocked quartz was derived from solid and porous Hugoniot experiments on silica,[35,37,38] and found to be essentially constant in the high-pressure fluid phase at $\Gamma = 0.6 \pm 0.1$.[39] This constant Gruneisen behavior is common among strongly shocked materials in the fluid regime and differs from the density-dependent Gruneisen typically observed at lower pressures in solids. Examining a range of EOS models for silica over the pressure range 4–17 Mbar applicable to this experiment, it was found that $\Gamma = 0.64 \pm 0.11$, in good agreement with experiment. The model-derived value and uncertainty are used in the analysis and are the only model-based parameters used in the impedance-matching calculations.

Systematic uncertainties in the impedance-matching analysis arise from uncertainties in three coefficients: a_0 and

TABLE I. Diamond-phase carbon Hugoniot results from impedance matching to a quartz standard. U_{sQ} and U_{sC} are the measured shock velocities in quartz and diamond with random (i.e., measurement) errors; values in curly brackets are the instantaneous acceleration of the shock velocity in km/s/ns at the impedance-matching instant. P_C (ran,sys), ρ_C (ran,sys), and U_{pC} (ran,sys) are the pressure, density, and particle velocity of shocked diamond inferred from impedance-matching calculations, showing both random and systematic errors. Random errors come from measurement uncertainties in U_{sQ} and U_{sC}, and systematic errors come from uncertainties in the principal and reshock Hugoniots of quartz. Shot numbers with an asterisk indicate targets with a thin quartz pusher; others had a thick quartz pusher.

Expt.	U_{sQ} km/s	U_{sC} km/s	P_C (ran,sys) Mbar	ρ_C (ran,sys) g/cm^3	U_{pC} (ran,sys) km/s
49976	17.29 ± 0.12 {−0.83}	20.39 ± 0.24 {0.45}	$6.25 \pm (0.09, 0.05)$	$6.14 \pm (0.09, 0.04)$	$8.73 \pm (0.11, 0.07)$
50364	18.83 ± 0.18 {−1.53}	21.66 ± 0.13 {−1.18}	$7.51 \pm (0.12, 0.07)$	$6.45 \pm (0.10, 0.05)$	$9.87 \pm (0.16, 0.09)$
49974	19.37 ± 0.10 {−0.99}	22.05 ± 0.11 {−0.05}	$7.96 \pm (0.07, 0.08)$	$6.58 \pm (0.06, 0.05)$	$10.28 \pm (0.09, 0.10)$
49614	19.96 ± 0.10 {−0.38}	22.46 ± 0.08 {−1.05}	$8.46 \pm (0.07, 0.08)$	$6.72 \pm (0.06, 0.06)$	$10.73 \pm (0.09, 0.11)$
51565	20.88 ± 0.12 {−2.72}	23.36 ± 0.07 {−0.87}	$9.34 \pm (0.09, 0.10)$	$6.85 \pm (0.07, 0.07)$	$11.40 \pm (0.10, 0.12)$
49616	20.94 ± 0.12 {−1.02}	23.46 ± 0.07 {−0.93}	$9.41 \pm (0.09, 0.10)$	$6.85 \pm (0.07, 0.07)$	$11.43 \pm (0.10, 0.12)$
49615	21.11 ± 0.11 {−1.36}	23.72 ± 0.07 {−1.02}	$9.60 \pm (0.08, 0.11)$	$6.83 \pm (0.06, 0.07)$	$11.54 \pm (0.09, 0.13)$
48882*	21.89 ± 0.11 {−4.25}	24.22 ± 0.07 {−1.45}	$10.32 \pm (0.09, 0.12)$	$7.03 \pm (0.06, 0.08)$	$12.14 \pm (0.10, 0.14)$
48448*	22.59 ± 0.12 {−3.83}	25.02 ± 0.09 {−1.84}	$11.08 \pm (0.10, 0.13)$	$7.08 \pm (0.07, 0.09)$	$12.62 \pm (0.11, 0.15)$
48880*	24.88 ± 0.06 {−2.32}	26.33 ± 0.07 {0.71}	$13.34 \pm (0.05, 0.17)$	$7.77 \pm (0.05, 0.12)$	$14.43 \pm (0.05, 0.18)$
49450*	27.63 ± 0.11 {−3.79}	28.42 ± 0.08 {−3.31}	$16.49 \pm (0.11, 0.23)$	$8.39 \pm (0.08, 0.16)$	$16.53 \pm (0.10, 0.23)$
49447*	29.74 ± 0.15 {−2.91}	30.19 ± 0.09 {−1.98}	$19.18 \pm (0.15, 0.30)$	$8.77 \pm (0.11, 0.20)$	$18.10 \pm (0.14, 0.28)$

a_1 from the quartz principal Hugoniot, and the Gruneisen parameter, Γ. These uncertainties are propagated throughout the analysis and combined in quadrature with the random uncertainties (arising from velocity measurements) to determine the total error. The relative importance of the various error contributions changes with shock pressure and will be described in the next section.

V. RESULTS

The results are listed in Table I and shown in both the U_s-U_p plane (Fig. 2) and the P-ρ plane (Fig. 3). The total uncertainty for these data is given by black error bars, corresponding to a quadrature sum of both random and systematic uncertainties; overlapping them, and always smaller, are a set of red error bars that correspond only to the random uncertainties. These data indicate an approximately linear U_s-U_p Hugoniot, which for reference is given (in units of km/s) by $U_s = (24.31 \pm 0.02) + (1.009 \pm 0.010)(U_p - 12.32)$. The errors in these coefficients are uncorrelated since the fit has been taken about the centroid of the data. In the standard form, this means that $U_s = 11.9 + 1.01 U_p$.

The total uncertainty in density, shown in Fig. 4, lies between 1.2 and 2.6% and is significantly smaller than the errors in previous laser-driven shock Hugoniot measurements. Total uncertainties in ρ_C (as well as P_C and U_C) were determined by the quadrature sum of five different sources of error: ΔU_{sQ}, ΔU_{sC}, Δa_0, Δa_1, and $\Delta\Gamma$. The first two are measurement errors while the last three are systematic errors in the quartz EOS. Examining these individual error contributions (see Fig. 4) it is apparent that below 10 Mbar the dominant uncertainty is from velocity measurement errors. At low velocities the VISAR is less precise since the constant error of 5% of a fringe is a larger fraction of the total velocity; also, below 10 Mbar, the reflectivity of the diamond shock front drops rapidly,[17] making the measurement of U_{sC} less precise. At higher pressures, the density errors due to velocity measurements begin to rise again slightly since the

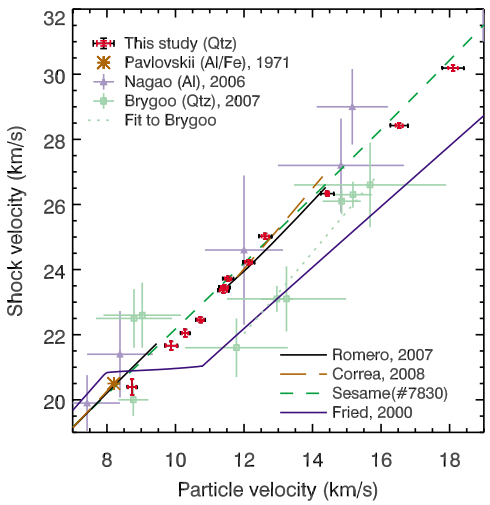

FIG. 2. (Color online) Shock velocity versus particle velocity plot of the diamond Hugoniot in and above the expected (Refs. 15 and 17) melt region (corresponding to $20 \lesssim U_s \lesssim 24$ km/s). Each data point from this study is given by a pair of overlapping error bars with the smaller errors (lighter colored) representing the random uncertainty and the larger errors representing the total uncertainty. These data are in general agreement with *ab initio* calculations from Romero and Mattson (Ref. 16) (black solid lines) and Correa *et al.* (Ref. 15) (brown long dashed lines) but disagree with previous measurements by Brygoo *et al.* (Ref. 21) (green squares) and with the free-energy model of Fried and Howard (Ref. 11) (blue solid lines). Our data are in general agreement with the data from Nagao *et al.* (Ref. 20) (blue triangles).

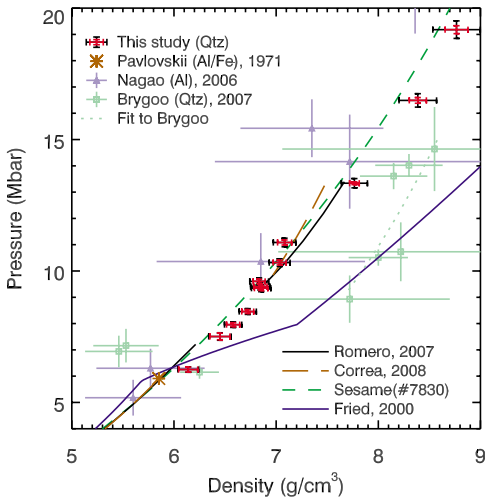

FIG. 3. (Color online) Pressure versus density plot of the diamond Hugoniot in and above the expected (Refs. 15 and 17) melt region (corresponding to $6 \lesssim P \lesssim 10$ Mbar). Each data point from this study is given by a pair of overlapping error bars with the smaller errors (lighter colored) representing the random uncertainty and the larger errors representing the total uncertainty. Other plot symbols and colors are the same as in Fig. 2.

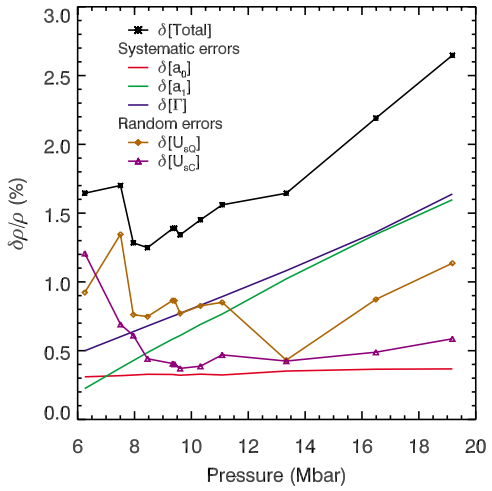

FIG. 4. (Color online) The total uncertainty in density is determined by a quadrature sum of three systematic components and two random components. Systematic errors arise from uncertainties in the quartz EOS as given by Hugoniot fit parameters (a_0 and a_1) and the Gruneisen parameter (Γ). Random errors arise from uncertainties in the shock velocities in quartz (δU_{sQ}) and diamond (δU_{sC}). Below ~10 Mbar, random errors dominate.

increased compression of diamond amplifies errors in the measured velocity; thus, despite the decrease in the velocity uncertainty itself, errors in density begin to increase again. Above 10 Mbar, systematic errors dominate. Precisely measuring the diamond Hugoniot above 20 Mbar using this technique will require improving the accuracy of the quartz standard.

The effects of preheat, shock curvature, and shock unsteadiness were considered but were found to be undetectable. Systematic shifts due to x-ray preheat were explored in the regime of 10 Mbar by examining data taken using either thin (~20 μm) or thick (~90 μm) quartz pushers. The latter provides >100 times the x-ray attenuation for x rays <4 keV. As shown in Table I, shots 48882 (thin pusher) and 49615 (thick pusher) both at pressures of ~10 Mbar have almost identical inferred densities. This indicates that, at least in this pressure regime and below, the effects of preheat on the measured compression are negligible.

Shock curvature can be a significant source of error for transit-time-based measurements across a step since breakout times are measured at spatially separated locations on the target; however, this is not a problem here since velocity measurements in both quartz and diamond were performed at the same point in space. Shock curvature could cause the VISAR to measure a velocity component that is less than the speed of the shock front. Based on the slightly curved breakout times across the target [shown in Fig. 1(b)], the largest incidence angles were ~2 degrees from normal. This would cause an error in the measured velocity of $\lesssim 0.1\%$.

Shock unsteadiness effects were investigated by checking for any differences between Hugoniot points taken at similar pressures but with varying degrees of shock steadiness. The measured accelerations of shock velocities in quartz and diamond at the impedance-matching instant are listed in curly brackets in Table I. From these data it can be seen that, for example, the quartz shock velocity acceleration on shot 59565 (−2.72 km/s/ns) is nearly three times that on shot 49616 (−1.02 km/s/ns) yet the Hugoniot points are almost identical. This is consistent with the argument presented in Sec. III that shock unsteadiness effects are not important in impedance-matching experiments as long as the velocities are taken at the instant the shock transits the interface between the two materials.

VI. DISCUSSION

These new high-precision measurements of the diamond Hugoniot directly overlap the pressure range explored in recent laser-driven shock experiments by Nagao *et al.*[20] and Brygoo *et al.*[21] Our new measurements are in general agreement with the data from Nagao *et al.*,[20] despite the large uncertainties in that previous study (see Sec. III). For proper comparison, we have reanalyzed those earlier data using an aluminum EOS that is in better agreement with available absolute Al Hugoniot data,[36] resulting in a slightly softer diamond Hugoniot than that reported originally by Nagao *et al.*[20] Data from experiments by Brygoo *et al.*[21] show a ~14% density jump at ~7.5 Mbar that was claimed as evidence for melting at a negative Clapeyron slope. Our measurements between 6 and 10 Mbar show no indication of such a large volume collapse.

Comparing our data with the lower-pressure measurements from Pavlovskii[18] does suggest the presence of a ~3% density increase at 6 Mbar, as shown in Fig. 3. This discontinuity appears to signify entry into the diamond-liquid coexistence regime as described below, although it could simply be an artifact of unknown experimental uncertainties (Pavlovskii did not report errors).

Hugoniot calculations based on the multiphase free-energy model of Fried and Howard,[11] which showed a dra-

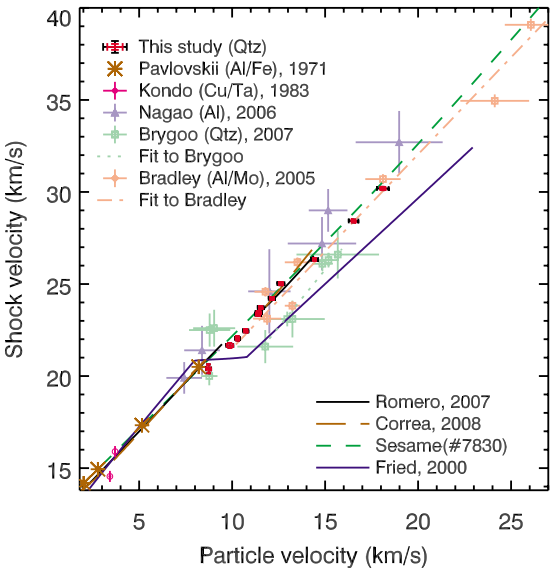

FIG. 5. (Color online) (See Appendix.) The diamond Hugoniot shown in Fig. 2 expanded to include unpublished measurements from Bradley *et al.* (Ref. 41) up to 36 Mbar. These data suggest that above 20 Mbar the Hugoniot still approximately follows the linear U_s-U_p fit found at lower pressures.

matic softening of the Hugoniot in the solid-liquid coexistence region, disagree with our measurements. It appears that the compressibility of the fluid in that model was too high, resulting in a large negative slope in the melting curve and, thus, an overly large density jump along the Hugoniot. A free-energy model from the SESAME (Ref. 40) database, which does not include multiple phases, disagrees slightly with our measurements between 6 and 10 Mbar but is in quite good agreement at higher pressures.

Ab initio predictions by Correa *et al.*[9,15] and Romero and Mattson[16] are shown in Figs. 2 and 3, with the gap in each line representing the implied coexistence region. Pavlovskii's data are in good agreement with the predicted solid Hugoniot, while our measurements are in agreement with the predicted liquid Hugoniot, at least up to the maximum calculated pressures of ~13 Mbar. This shows that the Hugoniots for the pure diamond and pure liquid phases almost fall along the same linear U_s-U_p relation.

Our measurements suggest that the solid-liquid coexistence regime has a slightly higher density (by 2%–3%) than would be expected from a simple interpolation between pure solid and liquid states. This mixed phase region between 6 and 10 Mbar is not calculated explicitly by the *ab initio* theories. Instead, the postulate of volume-weighted linear mixing, which assumes a homogenous mixture with negligible interfacial free energy, is commonly invoked to treat such a mixed region.[15] Additional complexity arises in the case of shock melting of diamond because the Hugoniot is predicted to pass through a BC8-liquid coexistence phase just before completion of melting, at around 9 Mbar.[15] More sophisticated calculations, beyond the linear mixing approximation, will be required to better understand how such mixed phases behave at high pressure.

VII. CONCLUSIONS

Precision measurements of the diamond Hugoniot between 6 and 19 Mbar have been used to probe carbon states in the dense, high-temperature fluid regime and along the diamond-liquid coexistence. These data, which represent a significant improvement over earlier laser-driven shock wave measurements on diamond, are in general agreement with recent *ab initio* model calculations of the diamond Hugoniot in the pure liquid phase from 10 to 13 Mbar and indicate a negative slope of melting with a few percent density increase. The extraordinarily large extent of the diamond-BC8-liquid coexistence regime between 6 and 10 Mbar may be a valuable way to test theories of how mixed phases behave at ultrahigh pressure.

ACKNOWLEDGMENTS

We thank the Omega operations crew for help in carrying out the experiments, Mark Bonino and the Omega target fabrication group for their outstanding work, and Walter Unites for his assistance throughout. This work was performed under the auspices of the U.S. Department of Energy by

TABLE II. (See Appendix.) Previously unpublished impedance-match Hugoniot data for diamond-phase carbon obtained using an aluminum or molybdenum reference standard. Subscript R refers to parameters of the reference standard and C of the sample. Columns indicate the initial density ($\rho_{0R,C}$), measured shock speed in the reference standard (U_{sR}) along with the nonsteadiness correction (ΔU_{sR}), measured shock speed in the sample (U_{sC}), and the inferred particle speed (U_{pC}), pressure (P_C), and density (ρ_C) in the diamond samples. Random and systematic uncertainties are listed separately for each quantity.

Expt.	ρ_{0R} g cm^{-3}	ρ_{0C} g cm^{-3}	U_{sR} km/s	ΔU_{sR} km/s	U_{sC} km/s	U_{pC} (ran,sys) km/s	P_C (ran,sys) Mbar	ρ_C (ran,sys) g cm^{-3}
20547(Al)	2.70	3.51	22.08 ± 0.75	0.00	23.12 ± 0.34	11.88 ± (0.74,0.09)	9.64 ± (0.060,0.008)	7.22 ± (0.50,0.06)
24278(Al)	2.70	3.51	22.28 ± 0.60	−1.28	24.58 ± 0.26	11.79 ± (0.58,0.09)	10.17 ± (0.051,0.008)	6.75 ± (0.32,0.05)
24365(Al)	2.70	3.51	23.59 ± 0.39	−0.16	23.82 ± 0.26	13.24 ± (0.39,0.11)	11.07 ± (0.033,0.010)	7.90 ± (0.33,0.08)
24294(Al)	2.70	3.51	24.36 ± 0.68	−0.12	26.18 ± 0.26	13.51 ± (0.67,0.12)	12.42 ± (0.062,0.011)	7.25 ± (0.40,0.07)
24288(Al)	2.70	3.51	29.92 ± 0.91	2.31	30.70 ± 0.27	18.11 ± (0.92,0.22)	19.52 ± (0.100,0.023)	8.56 ± (0.65,0.15)
20541(Al)	2.70	3.51	36.74 ± 1.76	0.83	34.95 ± 0.35	24.12 ± (1.82,0.34)	29.60 ± (0.220,0.040)	11.30 ± (1.90,0.40)
26397(Mo)	10.2	3.51	30.96 ± 0.92	0.58	39.08 ± 0.33	26.10 ± (1.11,0.88)	35.80 ± (0.150,0.120)	10.57 ± (0.92,0.72)

Lawrence Livermore National Laboratory in part under Contract No. W-7405-Eng-48 and in part under Contract No. DE-AC52-07NA27344, and by the University of Rochester under Cooperative Agreement No. DE-FC03-92SF19460.

APPENDIX

Prior to the experiments reported above, several of the present authors performed measurements of the diamond Hugoniot using an aluminum or molybdenum standard.[41] Shock velocities in the standard were determined using transit-time measurements (since both Al and Mo are optically opaque), while shock velocities in the diamond were determined using the VISAR. Diamond oriented along the (110) axis was used. In order to account for shock unsteadiness, the time-resolved measurements of the velocity history in diamond were used to infer the velocity history in the opaque standard. However, the limited precision of the transit-time measurement (as discussed in Sec. III) resulted in data with much larger error bars than those in the improved experiment described above.

A comparison of the two data sets shows that, despite the large random uncertainties, the fit to the less precise data is in quite good agreement with the new measurements (see Fig. 5). The best linear U_s-U_p fit to the data is given (in units of km/s) by $U_s=(25.73\pm0.30)+(1.054\pm0.090)(U_p-14.010)$ and is labeled on the plots as "Fit to Bradley." Since these older data include the highest diamond Hugoniot measurements ever performed (up to 36 Mbar), we include them here for reference (see Table II).

*Author to whom correspondence should be addressed: hicks13@llnl.gov

[1] "Melting, Boiling, Triple, and Critical Point Temperatures of the Elements," in *CRC Handbook of Chemistry and Physics*, 88th ed., edited by D. R. Lide (CRC, Boca Raton, FL/Taylor & Francis, London, 2008).
[2] F. P. Bundy, W. A. Bassett, M. S. Weathers, R. J. Hemley, H. K. Mao, and A. F. Goncharov, Carbon **34**, 141 (1996).
[3] M. T. Yin and M. L. Cohen, Phys. Rev. Lett. **50**, 2006 (1983).
[4] F. P. Bundy, J. Chem. Phys. **38**, 631 (1963).
[5] J. W. Shaner, J. M. Brown, C. A. Swenson, and R. G. McQueen, J. Phys. (Paris), Colloq. **45**, c8 (1984).
[6] D. A. Young and R. Grover, in *Shock Compression of Condensed Matter–1987*, edited by S. Schmidt and N. C. Holmes (North-Holland, Amsterdam, 1988), pp. 131–134.
[7] M. van Thiel and F. H. Ree, Int. J. Thermophys. **10**, 227 (1989).
[8] A. M. Molodets, M. A. Molodets, and S. S. Nabatov, in *Shock Compression of Condensed Matter–1997*, edited by S. C. Schmidt, D. P. Dandekar, and J. W. Forbes (American Institute of Physics, New York, 1998), p. 91.
[9] A. A. Correa, S. A. Bonev, and G. Galli, Proc. Natl. Acad. Sci. U.S.A. **103**, 1204 (2006).
[10] X. Wang, S. Scandolo, and R. Car, Phys. Rev. Lett. **95**, 185701 (2005).
[11] L. E. Fried and W. M. Howard, Phys. Rev. B **61**, 8734 (2000).
[12] M. P. Grumbach and R. M. Martin, Phys. Rev. B **54**, 15730 (1996).
[13] S. Fahy and S. G. Louie, Phys. Rev. B **36**, 3373 (1987).
[14] W. J. Nellis, A. C. Mitchell, and A. K. McMahan, J. Appl. Phys. **90**, 696 (2001).
[15] A. A. Correa, L. X. Benedict, D. A. Young, E. Schwegler, and S. A. Bonev, Phys. Rev. B **78**, 024101 (2008).
[16] N. A. Romero and W. D. Mattson, Phys. Rev. B **76**, 214113 (2007).
[17] D. K. Bradley, J. H. Eggert, D. G. Hicks, P. M. Celliers, S. J. Moon, R. C. Cauble, and G. W. Collins, Phys. Rev. Lett. **93**, 195506 (2004).
[18] M. N. Pavlovskii, Sov. Phys. Solid State **13**, 741 (1971).
[19] K. Kondo and T. J. Ahrens, Geophys. Res. Lett. **10**, 281 (1983).
[20] H. Nagao, K. G. Nakamura, K. Kondo, N. Ozaki, K. Takamatsu, T. Ono, T. Shiota, D. Ichinose, K. A. Tanaka, K. Wakabayashi, K. Okada, M. Yoshida, M. Nakai, K. Nagai, K. Shigemori, T. Sakaiya, and K. Otani, Phys. Plasmas **13**, 052705 (2006).
[21] S. Brygoo, E. Henry, P. Loubeyre, J. Eggert, M. Koenig, B. Loupias, A. Benuzzi-Mounaix, and M. Rabec Le Gloahec, Nature Mater. **6**, 274 (2007).
[22] T. R. Boehly, D. L. Brown, R. S. Craxton, R. L. Keck, J. P. Knauer, J. H. Kelly, T. J. Kessler, S. A. Kumpan, S. J. Loucks, S. A. Letzring, F. J. Marshall, R. L. McCrory, S. F. B. Morse, W. Seka, J. M. Soures, and C. P. Verdon, Opt. Commun. **133**, 495 (1997).
[23] L. M. Barker and R. E. Hollenbach, J. Appl. Phys. **43**, 4669 (1972).
[24] L. M. Barker and K. W. Schuler, J. Appl. Phys. **45**, 3692 (1974).
[25] P. M. Celliers, G. W. Collins, L. B. D. Silva, D. M. Gold, and R. Cauble, Appl. Phys. Lett. **73**, 1320 (1998).
[26] P. M. Celliers, D. K. Bradley, G. W. Collins, D. G. Hicks, T. R. Boehly, and W. J. Armstrong, Rev. Sci. Instrum. **75**, 4916 (2004).
[27] D. G. Hicks, T. R. Boehly, J. H. Eggert, J. E. Miller, P. M. Celliers, and G. W. Collins, Phys. Rev. Lett. **97**, 025502 (2006).
[28] On a single shot (48880) the 18-mm etalon was replaced by a 45-mm etalon.
[29] T. R. Boehly, D. G. Hicks, P. M. Celliers, T. J. B. Collins, R. Earley, J. H. Eggert, D. Jacobs-Perkins, S. J. Moon, E. Vianello, D. D. Meyerhofer, and G. W. Collins, Phys. Plasmas **11**, L49 (2004).
[30] T. R. Boehly, J. E. Miller, D. D. Meyerhofer, J. H. Eggert, P. M. Celliers, D. G. Hicks, and G. W. Collins, *Shock Compression of Condensed Matter—2007*, AIP Conf. Proc. No. 955 (AIP, Melville, NY, 2007), p. 19.
[31] J. Eggert, S. Brygoo, P. Loubeyre, R. S. McWilliams, P. M. Celliers, D. G. Hicks, T. R. Boehly, R. Jeanloz, and G. W. Collins, Phys. Rev. Lett. **100**, 124503 (2008).
[32] J. M. Walsh, M. H. Rice, R. G. McQueen, and F. L. Yarger, Phys. Rev. **108**, 196 (1957).
[33] Y. B. Zeldovich and Y. P. Raizer, *Physics of Shock Waves and High-Temperature Hydrodynamic Phenomena* (Dover, Mineola, NY, 2002).
[34] S. Brygoo, D. G. Hicks, P. Loubeyre, J. Eggert, R. S. McWill-

iams, P. M. Celliers, T. R. Boehly, R. Jeanloz, and G. W. Collins (unpublished).
[35] D. G. Hicks, T. R. Boehly, P. M. Celliers, J. H. Eggert, E. Vianello, D. D. Meyerhofer, and G. W. Collins, Phys. Plasmas **12**, 082702 (2005).
[36] P. M. Celliers, G. W. Collins, D. G. Hicks, and J. H. Eggert, J. Appl. Phys. **98**, 113529 (2005).
[37] R. F. Trunin, Phys. Usp. **37**, 1123 (1994).
[38] R. F. Trunin, *Shock Compression of Condensed Materials* (Cambridge University Press, Cambridge, 1998).
[39] Silica is a particularly valuable impedance-matching standard because of the ready availability of polymorphs with different initial densities. This allows an accurate determination of the Gruneisen parameter up to very high pressures.
[40] S. P. Lyon and J. Johnson, Los Alamos National Laboratory Technical Report No. LA-CP-98-100, 1998.
[41] D. K. Bradley, P. M. Celliers, J. H. Eggert, D. G. Hicks, D. H. Munro, and G. W. Collins (unpublished).